Design and Implementation of Wideband Spectrum Sensing on SDR Platform With Receiver Calibration

J. C. Merlano-Duncan[+], Tadilo Endeshaw Bogale[+], Long Bao Le[+],
Martin Turgeon[++], Jean-Benoit Larouche[++], and Rene Lamontagne[++]
Institute National de la Recherche Scientifique (INRS)[+]
Nutaq Incorporated[++]
Email: {juan.duncan, tadilo.bogale, long.le}@emt.inrs.ca,
{martin.turgeon, jb.larouche, rene.lamontagne}@nutaq.com

***Abstract*— This report examines detection algorithms and their implementations for wideband CR network using Nutaq SDR platform. The sensing design and implementation approach employs the algorithms of [1] which applies ratio based test statistics for detecting the edges of all sub-bands, energy comparison approach to reliably detect the reference white sub-band and generalized energy detection to detect each of the sub-bands other than the reference sub-band. In particular, this report compares the performances of these algorithms with and without performing calibration (which will be clear in the sequel) of the Nutaq SDR platform. Through extensive experiment we have found that performing receiver calibration is helpful to achieve the theoretical performances claimed by [1] reliably. Moreover, we also verify that the considered detection algorithms are indeed robust against noise variance uncertainty and do not suffer from SNR wall. And the performances of these algorithms will not be affected by carrier frequency offset and moderate interference signal, and achieve promising result in the real world scenario.**

I. Introduction:

With the popularization of high bandwidth wireless devices in our daily lives, the radio frequency spectrum has become a very precious resource. It is not unusual to find a geographical spot in which some frequency bands (i.e., WiFi bands) are so crowded. On the other hand, there are frequency segments that are inefficiently exploited and only used by regulated conventional networks (for example a public TV service). The concept of Cognitive Radio (CR) has been proposed as a solution to enable the reuse of the underutilized frequency bands in an opportunistic manner. One of the fundamental requirements of a CR device is its capability to discern the nature of the surrounding radio environment to exploit the available spectrum opportunities [2]. This is performed by the spectrum sensing function of the CR network.

Recently wideband spectrum sensing has received a lot of attention where the considered band has more than one sub-bands. Thus, in a wide band spectrum sensing, it is required to determine the number and bandwidth of sub-bands, and examine each of the sub-bands to verify whether it is occupied by the primary user (PU) or not. In [3], [4], the edge detection approach is applied to identify the edges of each sub-band. Once the edges of each sub-band is determined, each of the sub-bands is examined independently using the well know energy detector. The approach of these papers, however, does not provide any analytical approach to examine the performance of their edge detector as a function of signal to noise ratio (SNR). Furthermore, these papers apply the conventional energy detection algorithm directly by assuming that the minimum average power of all sub-bands is equal to the noise variance.

Recently a unified sensing and optimization framework is proposed in [1] (by NECPHY-Lab, INRS) for wideband CR networks with noise variance uncertainty. The paper proposes a simple ratio based edge detection algorithm to detect the edges of each sub-band. And for the given edge, new generalized energy detection algorithm is proposed. The performance of the edge detection and generalized energy detection algorithms of [1] have been quantified analytically as a function of SNR and are shown to be robust against noise variance uncertainty. Furthermore, this paper exploits the fact that "when the noise variance is estimated from a finite bandwidth, the theoretical results of the conventional energy detection algorithm can not be applied directly". The theoretical results of [1] are demonstrated by computer simulations. The work of this paper, however, does not provide experimental results to validate the theory.

The current report studies the algorithms of [1] and provides extensive experimental results using a commercial Software Defined Radio (SDR) platforms. In particular, we exploit the usefulness of performing receiver calibration prior to the signal detection phases. And we validate that performing simple receiver calibration helps to improve the detection performances of the system. Furthermore, the experimental results show that the analytical expressions shown in [1] can be obtained in a practical scenario, accurately meeting the theory.

This report is organized as follows. Section II discusses the system model and problem statement. The considered ratio based edge detection, reference white sub-band detection and generalized energy detection algorithms are discussed in Section III. In Section IV experimental results are presented for several practically relevant settings. Finally conclusions are drawn in Section V.

II. System Model and Problem Statement

Consider a wide band CR network that operates within a given bandwidth of B Hz where different sub-bands have

different power spectrum density (PSD).

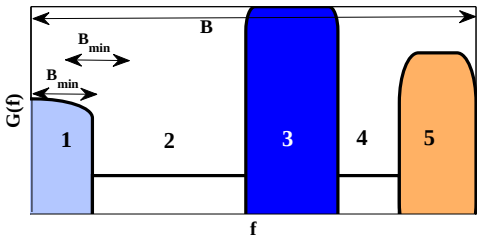

Fig. 1. The power spectral density of a wide-band signal comprising different sub-bands (SBs): SB_2 and SB_4 are white spaces.

Fig. 1 illustrates a typical utilization pattern of the spectrum where the number of sub-bands is 5. We assume that a cognitive device attempts to identify the available spectrum holes in order to perform transmission on these spectrum holes[1]. It is assumed that the considered wide-band contains one or more white sub-bands. This assumption is reasonable since according to the Federal Communications Commission (FCC) report, spectrum utilization on most available frequency bands is quite low [5]. And we consider that the CR network performs sensing and transmission repeatedly over equal frame intervals as shown in Fig. 2.

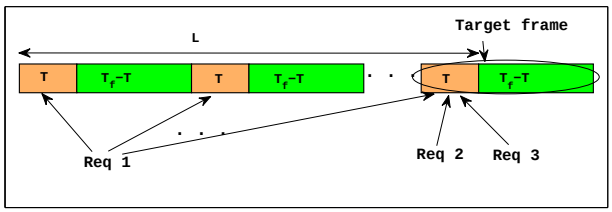

Fig. 2. The frame structure of a cognitive radio network.

As we can see from this figure, each frame of duration T_f has both sensing time (T) and data transmission time ($T_f - T$). The sensing time is required to reliably detect the white spaces of the considered wideband whereas, the data transmission time is required to execute data transmission on the white spaces. In practice T_f could be set as the channel evacuation time of the CR network. For example, T_f can be set to 2 second according to the 802.22 standard. We assume that the edges of each sub-band remain unchanged for L consecutive frames. This assumption is reasonable as boundaries of the sub-bands would not change very quickly. Therefore, L can be quite large in practice. However, in these frames, the PSD of each sub-band may change from one frame to another (i.e., a sub-band may contain noise only or signal plus noise in two consecutive frames). Under these practically valid assumptions, the wideband sensing design addresses the following requirements:

Req 1: Detecting the edges of each sub-band from the received samples of the current frame and previous $L-1$ frames (i.e., This requirement will employ the samples of duration LT seconds).

Req 2: Determining the reference white sub-band from the received samples of each frame which depends on T (i.e., the sub-band which contains noise only). This step is required to estimate the noise variance from the reference white sub-band.

Req 3: Detecting each of the remaining sub-bands (i.e., sub-bands other than the reference white sub-band) using the noise variance obtained from **Req 2** and the received samples of each frame which depends on T.

In particular, this report examines the effect of L and T on the performance of the edge detection (i.e., **Req 1**), and the effect of T on the performances of **Req 2** and **Req 3** using the Nutaq SDR platform (see fig. 2).

Note that in Fig. 2, the target frame (i.e., L) utilizes the samples of the previous $L-1$ frames and its own frame. As will be clear later, it is still possible to perform edge detection just from the current frame. However, such approach will not ensure reliable results. Due to this fact we utilize the samples of the previous L frames for our edge detector. By doing so, we are able to identify the edges of each sub-band without any error. From this figure, one can understand that any frame i will utilize the received samples of the frames $i-(L-1)$ to i.

III. Wideband Spectrum Sensing

Suppose that a given wideband of B Hz is examined to determine the available spectrum sub-bands. In each frame, the baseband received signal after down-conversion is expressed as:

$$r(t) = s(t) + w(t), \qquad 0 \le t \le T. \tag{1}$$

After sampling this signal with a sampling rate of B Hz (i.e., Nyquist sampling rate), the sampled version of $r(t)$ can be expresses as

$$r[n] = s[n] + w[n], \qquad n = 1, \cdots, N \tag{2}$$

where $N = TB$ is the number of received samples in the sensing time T. It is assumed that $w[n]$ for all n are independent and identically distributed (i.i.d) zero mean circularly symmetric complex Gaussian (ZMCSCG) random variables all with variance σ^2 which is unknown or known imperfectly. In the following subsections, the edge detection, reference white sub-band isolation and generalized energy detection algorithms proposed in [1] will be discussed briefly.

A. Edge Detection Algorithm

Consider a frequency in the PSD which lies in the boundary between noise only and signal plus noise regions (i.e., an edge of the two neighboring sub-bands). As the PSD of the noise only region is different from that of the signal plus noise region, this frequency point corresponds to an edge. Thus, any candidate frequency can be labeled as edge or not-an-edge just by comparing the PSDs of its right and left frequency regions each of which has size $\frac{B_{\min}}{2}$ since the minimum bandwidth of each sub-band is $B_{\min}$. Obviously, if these two PSDs are

[1]A CR network is a network that does not have exclusive right to use this wide-band. It is always termed as a secondary network.

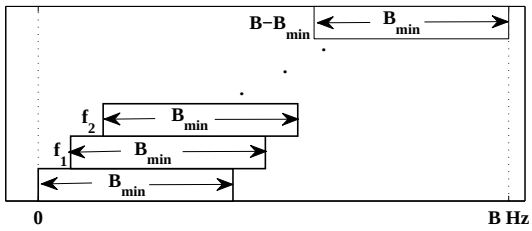

Fig. 3. Slided frequency regions for the edge detection algorithm.

significantly different, the candidate frequency is treated as an edge otherwise it is not an edge. This fact is apparently seen from Fig. 1. This motivates [1] to propose a simple ratio test to identify the edges of a wideband signal. In the following, we provide a brief explanation of the ratio based edge detection [1].

All the edges of the wide-band can be identified using the aforementioned idea by sliding the desired frequency region of size B_{min} as illustrated in Fig. 3 where an edge location results in the corresponding local maximum of the test statistics. Here, the offset between two consecutive examined frequency regions can be set according to the resolution of the discrete time Fourier transform (DFT) of received time-domain signal samples. In other words, the existence of edges in frequency regions $[f_i : f_i + B_{min}], \forall f_i \in [0,\ B - B_{min}]$ can be verified by computing the test statistics where the frequency resolution $f_i - f_{i-1}$ can be set according to the DFT resolution.

It is understood that the ratio based edge detection algorithm depends on the PSD of the received signal. The PSD of the received samples can be obtained using the DFT approach as follows. The discrete Fourier transform (DFT) of $r[n]$ is given as

$$\tilde{r}[m] = \sum_{n=1}^{N} \frac{r[n] \exp^{\frac{-i2\pi(m-1)(n-1)}{N}}}{\sqrt{N}}, \quad m = 1, \cdots, N. \quad (3)$$

By defining $\Delta f \triangleq \frac{B}{N}$, the PSD $G(f)$ of Fig. 1 and $\tilde{r}[m]$ are related as

$$G(f) \triangleq |\tilde{r}[m]|^2, \quad (m-1)\Delta f \leq f \leq m\Delta f, \quad \forall m.$$

Now any candidate frequency f_c is classified as edge or not-edge by examining the average energies of the frequency regions $[f_c : f_c + B_{minh}]$ and $[f_c : f_c - B_{minh}]$, where $B_{minh} = \frac{B_{min}}{2}$. In the following, we provide the detailed edge detector to check whether there is an edge or not when $f_c = B_{minh}$ (the same approach can be applied for the other candidate frequencies). For this f_c, the left and right side frequency regions are $[0 : B_{minh}]$ and $[B_{minh} : B_{min}]$, respectively. And the average energies (AE) of these frequency regions can be given as

$$\mathrm{AE}([0 : B_{minh}]) = \sum_{m=1}^{N_h} \frac{|\tilde{r}[m]|^2}{N_h} \triangleq \sum_{j=1}^{N_h} \frac{|v[j]|^2}{N_h} \triangleq \hat{M}_v \quad (4)$$

$$\mathrm{AE}([B_{minh} : B_{min}]) = \sum_{m=1}^{N_h} \frac{|\tilde{r}[N_h + m]|^2}{N_h} \triangleq \sum_{j=1}^{N_h} \frac{|\tilde{v}[j]|^2}{N_h} \triangleq \hat{M}_{\tilde{v}}$$

where $N_h = \lfloor B_{minh} T \rfloor$, $\{v[j] = \tilde{r}[m]\}_{j=m=1}^{N_h}$ and $\{\tilde{v}[j] = \tilde{r}[N_h + m]\}_{j=m=1}^{N_h}$.

For each frame, to check whether f_c is an edge or not, the following test statistics has been used [1].

$$\tilde{R}_e = \sqrt{\frac{N_h}{2}} \left(\frac{\hat{M}_v}{\hat{M}_{\tilde{v}}} - 1 \right). \quad (5)$$

As justified in the previous section, since the edges of each sub-band remains constant for L frames, we modify the test statistics (5) as

$$R_{eL} = \sum_{i=1}^{L-1} \tilde{R}_{ei}^2 \quad (6)$$

where $\tilde{R}_{ei}$ is $\tilde{R}_e$ of (5) corresponding to the ith frame. The P_d and P_f of this test statistics can be found in [1] (see [1] for more details).

B. Reference White Sub-band Detection

This subsection discusses the reference white sub-band detection approach. Suppose that we have identified the edges of each sub-band (i.e., **Req 1**). The next objective will be to reliably detect the reference white sub-band (i.e., **Req 2**). We propose to choose the sub-band that has the *least average energy* to be the *reference white sub-band*. If SB_i is chosen as a reference white sub-band and $SB_k, k \neq i$ are other sub-bands that may contain signal plus noise, **Req 2** is accomplished when we ensure $\mathrm{AE}(SB_k) \geq \mathrm{AE}(SB_i), \forall k \neq i$ which can be achieved by comparing the AE of all the available sub-bands.

C. Generalized Energy Detection

The number of sub-bands are determined from **Req 1** and the reference white sub-band is identified from **Req 2**. Now the remaining task will be to label each of the sub-bands as white or not. As explained previously, the considered band contains at least one white sub-band. Thus, we consider that the reference white sub-band SB_i obtained from **Req 2** contains only noise signal. For better exposition of the generalized energy detection, suppose that B_j is the bandwidth of the sub-band j with $\sum_{j=1}^{S_{sb}} B_j = B$, where S_{sb} is the number of sub-bands. We assume that SB_i is the reference sub-band and $SB_k, k \neq i$ are the target sub-bands which needs to be checked whether each of them is white or non white.

Now, to detect the kth sub-band, the following test statistics is applied [1]

$$R_k = \sqrt{\frac{N_{dk}\beta_k}{\beta_k + 1}} \left(\frac{\mathrm{AE}(SB_k)}{\mathrm{AE}(SB_i)} - 1 \right), \qquad \forall k \neq i \quad (7)$$

where $\beta_k = \frac{B_i}{B_k}$ and $N_{dk} = \lfloor T B_k \rfloor$. The detailed P_d and P_f of this test statistics can be obtained in [1].

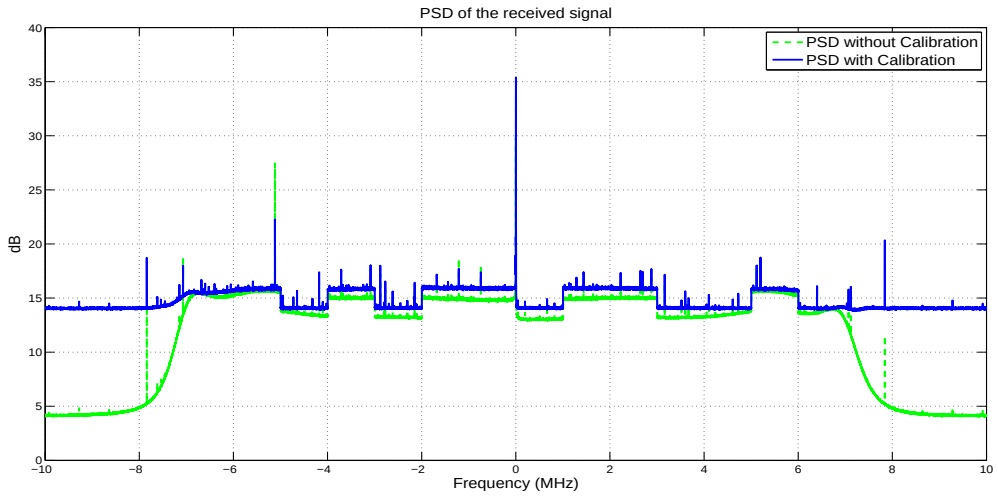

Fig. 5. Sample power spectral density at SNR=-3dB: [Green] Without calibration, [Blue] With calibration.

.

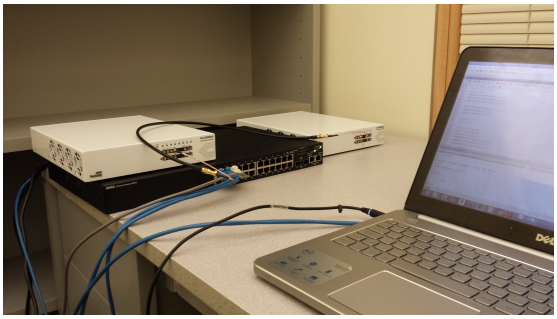

Fig. 4. The experimental setup used in this paper.

IV. Experimental Results

This section discusses experimental results of the edge detection, reference white sub-band detection and generalized energy detection algorithms. The implementation was performed using a pair of SDR devices, in particular the PicoSDR platform produced by Nutaq Incorporated. One SDR device was used to emulate multiple transmitters and the second SDR was the cognitive device which implemented the spectrum sensing. These two SDRs and the laptop are connected through an Ethernet switch. To exploit the additive white Gaussian noise (AWGN) channel, the two SDRs are directly connected to each other through SMA cable as shown in Fig. 4. The transmitted signal was composed of a set of subbands each with 1MHz bandwidth generated at a sampling rate of 20MHz using complex samples, in a center frequency of 2.99GHz. This signal is obtained from an OFDM modulation which uses 16384 frequency subcarriers for the complete 20MHz bandwidth. All the subcarriers are modulated by QPSK symbols that are generated randomly. The carriers inside a set of arbitrary selected subbands are multiplied by zero in order to generate the desired white spaces in frequency. Finally the FFT algorithm is applied to obtain the time samples which are upconverted in the SDR device. The amplitude of the transmitted signal is controlled in baseband and also using the RF amplification parameters of the PicoSDR device.

In reception the other PicoSDR receives the RF signal through a coaxial cable and downconverts it using a 2.99 GHz local oscillator. A baseband filter frequency is chosen among the available frequencies of the SDR device. Thus we have chosen the highest frequency which in this case was 7 MHz. After that, the baseband IQ signal is digitalized at a rate of 20 MHz, and are stored in the RAM memory positions of the device.

A. Sample Power Spectral Density

For better exposition of the experimental section, let us examine the PSD of the received signal. Fig. 5 shows the sample spectrum taken by averaging 100 experiments. The PSD of the received signal with the OFDM pattern after filtering is shown in Fig. 5 (i.e., without calibration). The magnitude of this PSD is shown in dB which is computed by examining the received signal samples in 16 bit integer value. In fact, there are some noticeable peaks around 0 and -5.11MHz. However, these frequency points are not from the actual transmitted signal. As we can see from this figure, when a sub-band does not contain any primary signal (i.e., under H_0 hypothesis), the received signal does not have flat spectrum. This is because of the following main reasons:

1) **Non flat transfer function of the filter**: The frequency response of any practical filter does not have an exact flat spectrum (both the transmitter and receiver).
2) **Spur signal**: Many of the electronic equipments have some spur signals. This arises from leakages of local oscillator, Crystal oscillator and ADC and DAC (from both the transmitter and receiver).
3) **Phase noise**: This is one of the most common challenges of most oscillators (both transmitter and receiver oscillators).

As can be seen from (2), to reliably ensure the desired performance of the proposed detectors, the noise signal should

have flat PSD (i.e., it should be white). Thus, before we perform any detection, we pre-process the received data to ensure that the received signal has (almost) flat PSD when there is no primary transmitter. This pre-processing step is literary termed as receiver calibration.

B. Receiver Calibration

As discussed above, in fact calibration is an important step for both at the transmitter and receiver. However, in CR network the transmitter and receivers are administered by different operators. Thus, performing calibration at both ends is not practical. For this reason, we propose to do calibration only at the Cognitive receiver (i.e., at the spectrum sensing device). To alleviate the effect of non flat transfer function of the filter, first we model the transfer function of the receive filter by the most commonly used polynomial function[2]. Then, we apply the computed coefficients to compensate the non-flat behavior of the receive filter. To remove the effect of spur and phase noise, we utilize signal cancellation approaches by equivalently express the spur and phase noise components using complex sinusoidal terms (See Fig. 5 (with calibration)). As will be clear in the sequel, performing calibration (even only at the receiver) achieves better detection performance compared to the scenario where there is no calibration.

C. Edge Detection

In this experiment we present the performance of the edge detection algorithm. To this end, we examine the effects of T on the performance of the edge detector test statistics (6). In order to estimate the operating SNR which is 0dB in this experiment, we examine the noise seen at the receiver. This is done by making an acquisition with the receiver radio frequency (RF) port disconnected. After this, we compute an average noise power for all the subbands which are inside the passband of the low pass filter used for the acquisition. The cutoff frequency of our low pass filter is set to 7MHz. Therefore, for all plots of this report, the frequency sections that are outside of the -7MHz to 7MHz intervals are not considered for evaluation purposes.

Fig. 6 shows the edge detection test statistics R_{eL} versus frequency for different sensing times with and without receiver calibration. From this plot, we can see that the magnitude of (6) increases as T increases. As a local maximum of the test statistics R_{eL} indicates the corresponding edge (i.e., either rising or falling edge), this result exploits the fact that increasing T will improve the detection performance of the edge detector which is expected. On the other hand, as discussed previously, there was a spur signal around -5.11MHz. And the detector without calibration has high amplitude at this frequency region whereas, the detector with calibration has low amplitude at this frequency region which is desirable as this region indeed does not contain an edge. On the other hand, the region around 7MHz also does not contain any edge. But we have observed very high peak at this frequency region when we perform edge detector without calibration. However, the edge detection with calibration exploits the fact that this frequency region is indeed not an edge. From this explanation, we can understand that performing receiver calibration is advantageous. Nevertheless, still since we perform calibration only at the receiver side we are not able to remove all the undesired peaks that arise from the joint effect of both the transmitter and receiver (for instance around the DC value of this figure).

[2]Note that the transfer function of most electronic filters can be well modeled by polynomial function with order in between 10 and 20. And for the Nutaq SDR device, we have used order 16.

D. Reference Sub-band Selection and Generalized Energy Detection

In this experiment, we examine the performance of the reference white sub-band and generalized energy detection for different scenarios with and without calibration. In this regard, we consider the reference sub-band as the sub-band with frequencies $3-5$MHz (i.e., our reference white sub-band). We discuss the effect of T (the sensing time) on the performance of these two detectors with and without calibration. Fig. 7 shows the test statistics R_k of (7) for different sub-bands and different sensing time T over a large number of realizations. We also show the detection threshold. Recall that a sub-band is considered to be white (i.e., available for cognitive network) if the corresponding test statistics is below the threshold and vice versa. The figure shows that we can successfully identify all white spaces. On the other hand, as expected, the variation in the average power (both in noise only and signal plus noise scenarion) decreases when we perform calibration.

From this figure, we can observe that R_k increases as the sensing time T (or the bandwidth of the considered band increases for fixed T) increases when there is a signal plus noise. However, in the noise only case, R_k remains almost the same especially with calibration. This is due to the fact that under the noise only case, each of the sub-bands has the same statistical behavior (i.e., $\mathcal{N}(0,1)$) whereas, increasing either T or the bandwidth increases the mean of R_k whenever there is a primary transmitted signal. From this result we can understand that for a given threshold (i.e., a constant P_f), the P_d of the generalized energy detector increases as T (bandwidth increases for fixed T) increases which is expected.

V. Conclusions

In this report, we consider sensing design and their implementations for wideband CR network using Nutaq SDR platform with and without receiver calibration. The sensing design and implementation approach employs the algorithms used in [1] which applies ratio based test statistics for detecting the edges of all sub-bands, simple energy comparison approach to reliably detect the reference white sub-band and generalized energy detection to detect each of the sub-bands other than the reference sub-band. The considered detection algorithms are robust against noise variance uncertainty and do not suffer from SNR wall and are tested in a practical environment. These algorithms achieve promising results in the real world scenario.

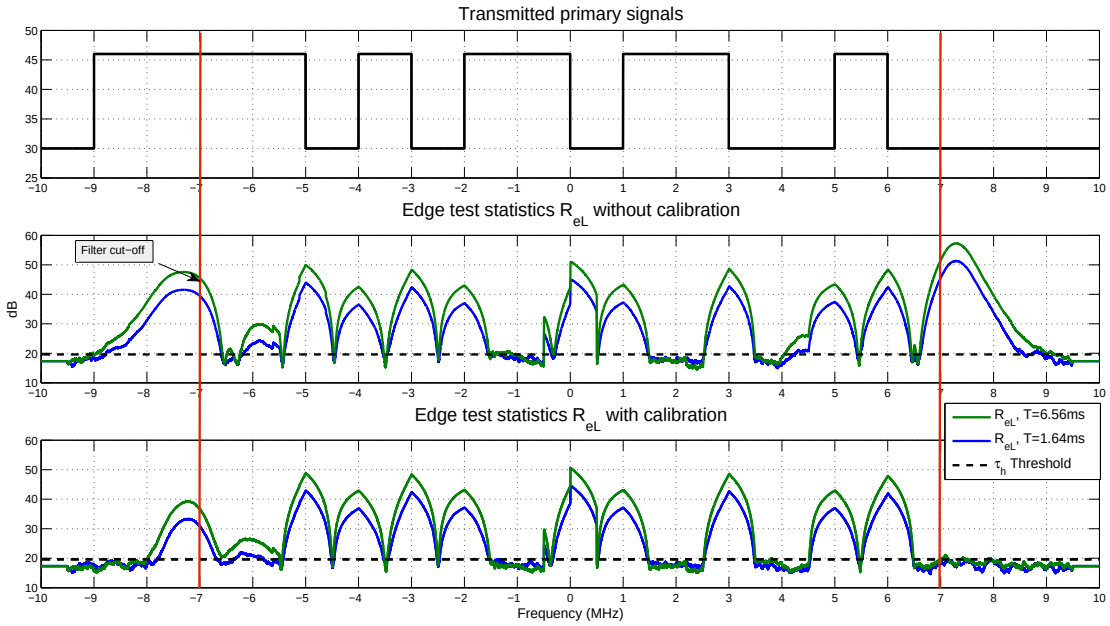

Fig. 6. The edge detector test statistics R_{eL} with $L = 54$, $SNR = 0$dB and different sensing time T with and without receiver calibration.

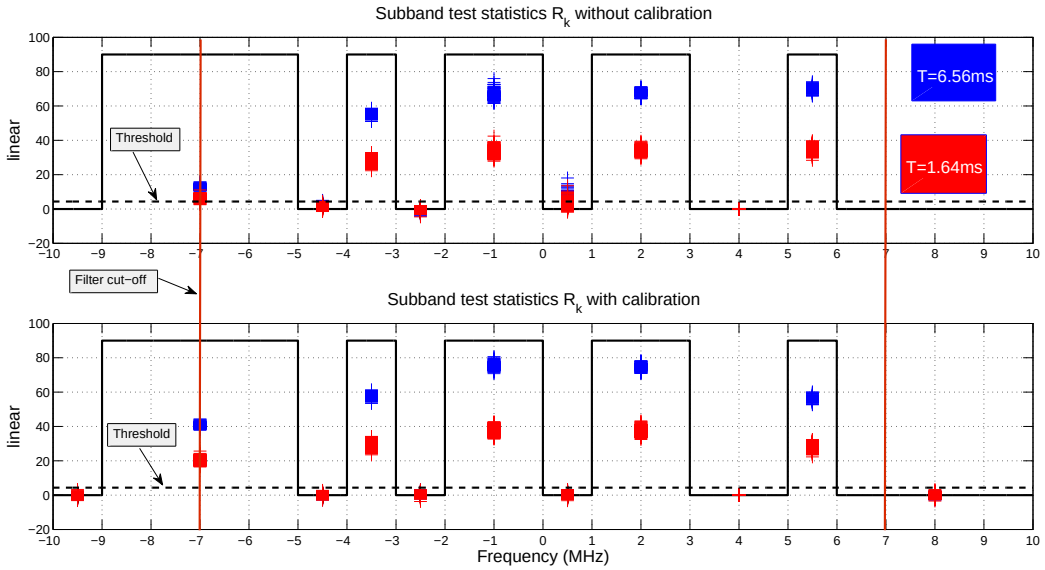

Fig. 7. The test statistics of the generalized energy detector R_k at $SNR = 0$dB and different sensing time T. The frequency [3MHz to 5MHz is selected as a reference sub-band.

REFERENCES

[1] T. E. Bogale, L. Vandendorpe, and L. B. Le, "Wideband sensing and optimization for cognitive radio networks with noise variance uncertainty," *IEEE Trans. Commun. (submitted)*, 2014.

[2] T. Yucek and H. Arslan, "A survey of spectrum sensing algorithms for cognitive radio applications," *IEEE Commun. Surveys Tutorial*, vol. 11, no. 1, pp. 116 – 130, 1st Quarter 2009.

[3] Y. Hur, J. Park, W. Woo, K. Lim, C. H. Lee, H. S. Kim, and J. Laskar, "A wideband analog multi-resolution spectrum sensing (MRSS) technique for cognitive radio (CR) systems," in *Proc. IEEE International Symposium on Circuits and Systems (ISCAS)*, May 2006, pp. 4090 – 4093.

[4] Z. Tian and G. B. Giannakis, "A wavelet approach to wideband spectrum sensing for cognitive radios," in *Proc. IEEE Cognitive Radio Oriented Wireless Networks and Communications (CROWNCOM)*, June 2006, pp. 1 – 5.

[5] I. F. Akyildiz, W. Lee, M. C. Vuran, and S. Mohanty, "Next generation/dynamic spectrum access/cognitive radio wireless networks: A survey," *ELSEVIER Journal Computer Networks*, vol. 50, no. 13, pp. 2127 – 2159, Sep. 2006.